Measurement of Biomechanical Properties of Tissues Under Uniaxial Stress

UNIVERSITY OF MINNESOTA Driven to Discover℠

Ashish Singal[1,2], Charles L. Soule[2], Seth Johnson[5], Daniel Keefe[5], Paul A. Iaizzo[1-4]

Departments of Biomedical Engineering[1], Surgery[2], Integrative Biology & Physiology[3], Institute of Engineering in Medicine[4], Computer Science & Engineering[5], University of Minnesota

The Visible Heart® Laboratory
Lab Focus: Translational Systems Physiology

INTRODUCTION

- Knowledge of biomechanical properties of tissues is necessary for credible description of their constitutive behavior in physiological conditions of normality and stress
- A comprehensive and comparative understanding of tissue properties is of prime importance from the perspectives of device-tissue interactions
- Moreover, ablation has become a common medical procedure, which alters both the structure and function of the ablated tissue; and in small percentage of cases, it can cause collateral damage of surrounding vital structures, which can have severe clinical implications
- In order to maximize the efficacy of ablative procedures and minimize collateral damage, it is important to understand the biomechanical properties of all tissues that may be potentially affected by ablation
- We have developed unique methodologies to assess the biomechanical properties of various tissues under uniaxial stress that include measurement of force-displacement graphs, stress-strain characteristics, calculations of avulsion forces, avulsion strains, energies associated with avulsions, and the elastic moduli of various tissue samples

METHODS

Tissue Preparation and Making of Tissue Bundles

- Fresh tissue samples were obtained from castrated male Yorkshire-cross swine and humans *(tissue deemed not transplantable or waste tissue)*
- Samples included cardiac trabeculae, pericardium, aorta, esophagus (muscularis and squamous epithelium), diaphragm, lungs, trachea, vastus lateralis, and rectus abdominus
- Tissue biopsies were dissected in oxygenated, temperature controlled Krebs-Ringers solution
- Excess fat and surrounding connective tissue was removed from each tissue, so that well-defined tissue bundles could be prepared
- Each bundle was dissected in a way to give it a dog-bone shape for added strength at both extremities
- In addition, liquid super-glue (cyanoacrylate) was applied on either ends of the tissue bundle at the suture-tissue interface; which allowed for added support, enhanced grip, and increased bonding strength at an otherwise vulnerable location
- Tissues such as diaphragm, rectus abdominus, vastus lateralis, cardiac trabeculae, and squamous epithelium were dissected in cylindrical shape having lengths of 20 to 25mm, and diameters of 2 to 5mm
- Tissues such as aorta, esophagus (muscularis), trachea, and pericardium were dissected in cuboidal shape having lengths of 20 to 25mm, widths of 2 to 5mm, and thicknesses of 0.25 to 3mm
- Bundles were tied on both ends with 2-0 silk sutures with a free loop on either ends so that they could be mounted on the uniaxial pull machine

Uniaxial Stress Testing

- Uniaxial pull testing (tensile strength measurements) was performed to assess biomechanical properties of various tissues
- Digital uniaxial force measurement system (Chatillon TCD 110 Series)
- 2 versatile force transducers (load cells): (1) maximum force of 10 N (accuracy: 0.01 N, resolution: 0.001 N); (2) maximum force of 100 N (accuracy: 0.1 N, resolution: 0.01 N)
- Pull protocol designed after gaining experience from conducting many pilot studies on different tissue samples, and conducting extensive literature search
- Tissues have been modeled as viscoelastic materials in this study
- Tissues were excised from the animal within a short time (less than two hours)
- Testing was performed at room temperature (22.5 ± 2°C)
- Uniqueness of this protocol is that it allowed for a slow, yet controlled pull of samples until avulsion occurred (tissue tears apart)
- Pull protocol was selected as having a constant speed of 10 mm/minute, or a strain rate of 0.167 s^{-1} over the avulsion stretch
- During execution, the system console display screen provided monitoring of 3 quantities, i.e. the load (N), stretch distance (mm), and speed (10 mm/min)
- Data was digitally acquired at a sampling rate of 100 Hz and saved to the hard drive for post-processing

Force-Displacement Measurements

- Once super-glue dried (<2 min), tissue samples were mounted on the pull machine via custom designed hooks of stainless steel material (needle of polypropylene sutures, Ethicon)
- The bottom suture loop was secured to the lower immobile hook mounted on the vice and the top suture loop was fixed to the uniaxial pull machine's force transducer as illustrated in **Figure 1**
- All tissue samples were stretched along the longitudinal axis of the sample until the sample avulsed
- Before starting the pull tests, initial lengths and diameters (for cylindrical samples), and initial lengths, widths, and thicknesses (for cuboidal samples) were recorded; to allow for the determination of the elastic modulus of each sample using the following equation/calculation:
- Elastic Modulus (EM) = Stress / Strain (N/m^2)
- Stress = Force / Area = F/A (N/m^2)
- Strain = Change in length / Original length = $\Delta l/L$
- Therefore, EM = $(F/A) / (\Delta l/L) = (F/\Delta l) \times (L/A)$

Figure 1. *Chatillon digital force measurement system to measure tensile strength characteristics of different tissues.* ***T:*** *A human esophagus muscle bundle is shown undergoing tensile strength test.* ***C:*** *System console to control the operation of instrument.* ***F:*** *Force transducer (load cell) with 10N maximum load capacity with a resolution of 1 mN.* ***UH*** *and* ***LH:*** *Custom designed upper and lower tissue holders hooks. Upper hook is connected to the force transducer and lower hook is held firmly to the vice as tissue is pulled to measure tensile strength of muscle bundle sample under test.*

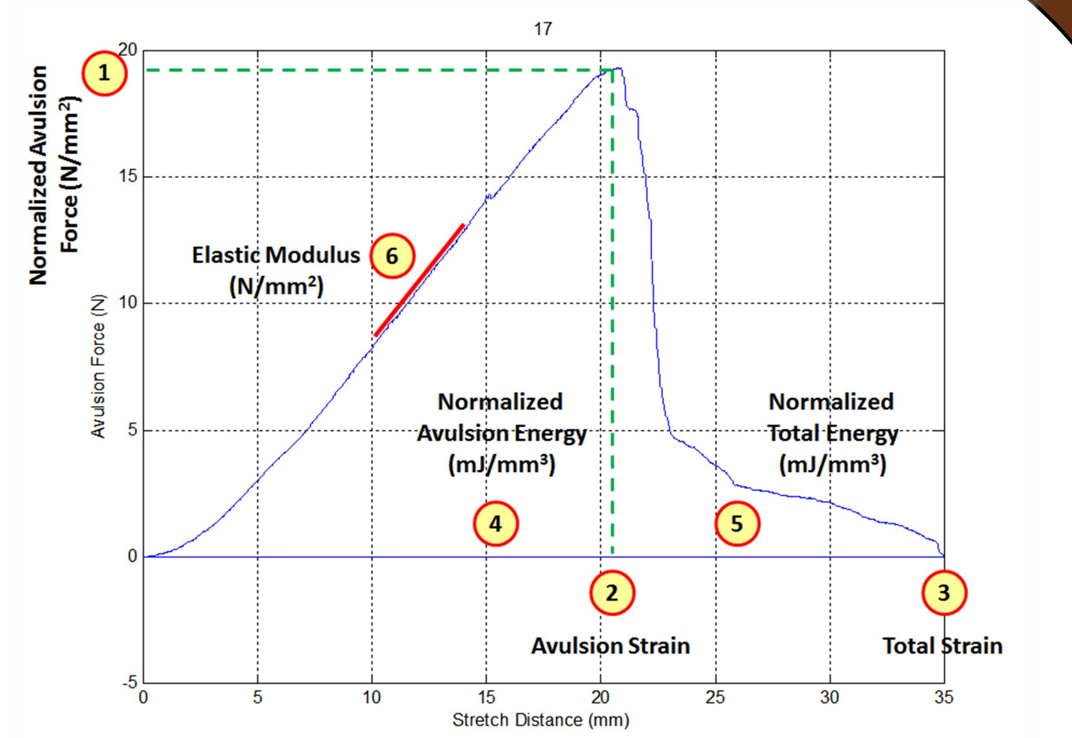

Figure 2. *A representative example showing the force-stretch characteristic of human pericardium. Six different quantities as mentioned on the graph are calculated for each sample. Avulsion force data was normalized to the cross-sectional area, and avulsion energy data was normalized to the volume of each tissue sample.*

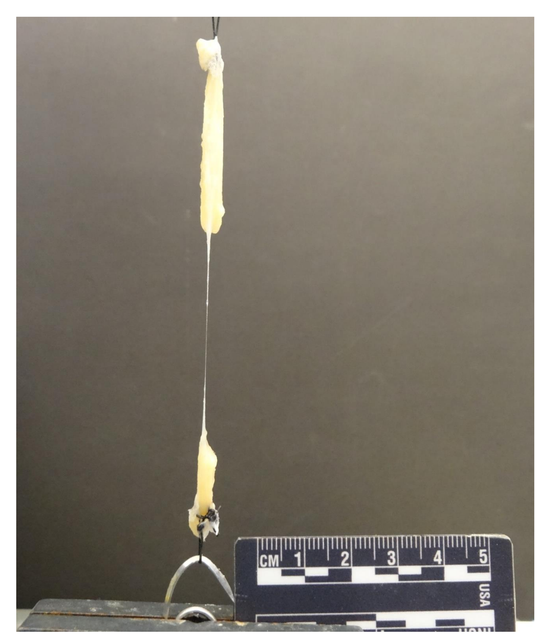

Figure 3. *A representative example illustrating center avulsion of human esophagus muscle bundle.*

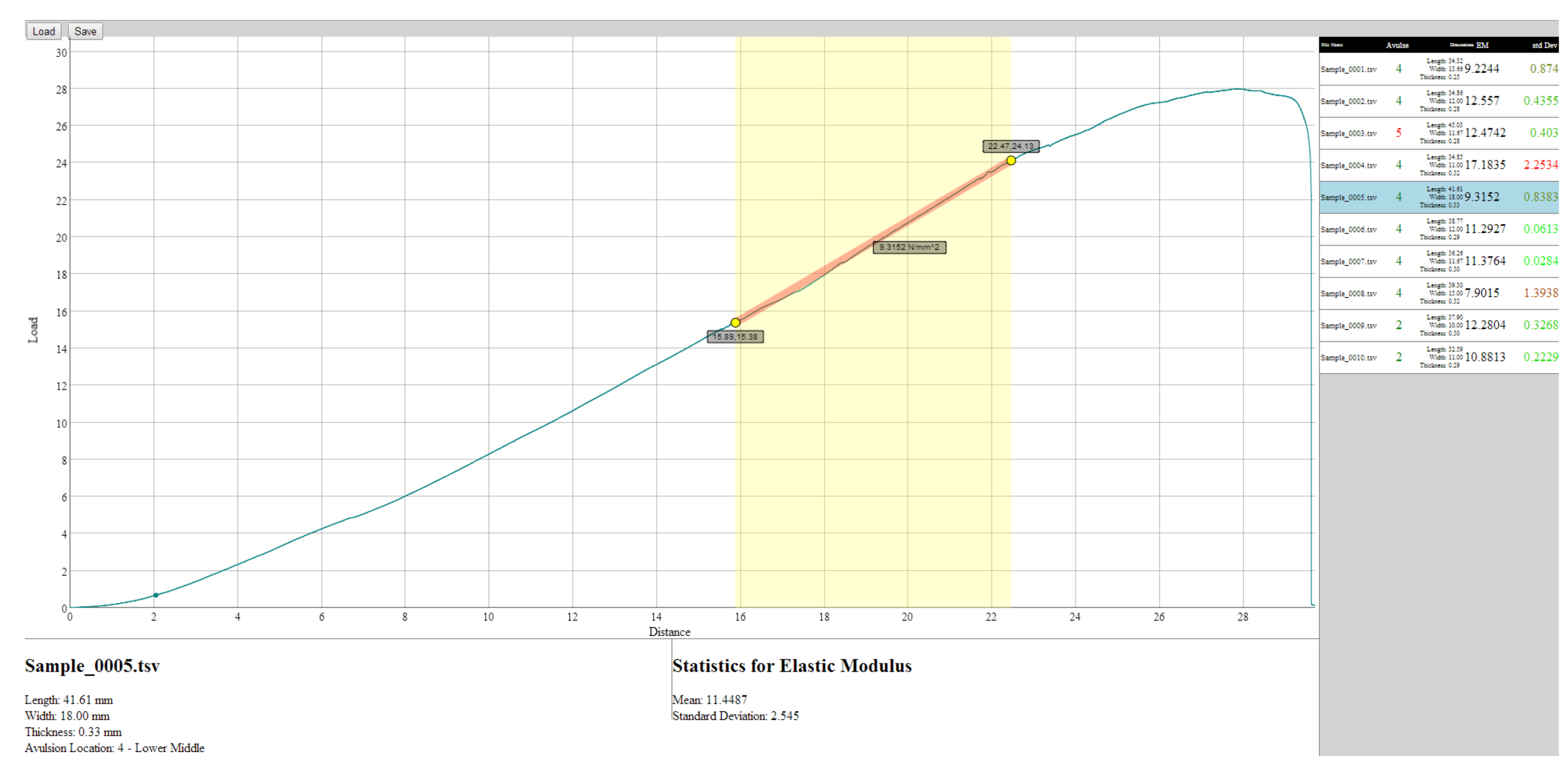

Figure 4. *A custom designed software application was written that allowed determination of elastic moduli of tissues. A representative example of human pericardium is shown with its dimensional characteristics and elastic modulus.*

1	Tissue #	Tissue Type	Total Samples	Mean Avulsion Force	Std Avulsion Force	Mean Avulsion Strain	Std Avulsion Strain	Mean Total Strain	Std Total Strain	Mean Avulsion Energy	Std Avulsion Energy	Mean Total Energy	Std Total Energy	Mean Elastic Modulus	Std Elastic Modulus
2	1	AceticAcid-Ablated Human Vastus Lateralis	2	0.0669	0.0041	0.4204	0.0027	0.4676	0.0260	4.6852	0.7878	6.0207	1.0980	0.4678	0.1426
3	2	AceticAcid-Ablated Swine Diaphragm	16	0.2517	0.0804	0.6070	0.1743	0.8932	0.2295	49.3375	18.8927	69.8646	25.7516	0.4682	0.1487
4	3	AceticAcid-Ablated Swine Esophagus	16	0.6680	0.1933	1.0414	0.2337	1.5526	0.2334	169.1670	55.6216	221.1098	59.2312	1.0084	0.3899
5	4	Cryo-Ablated Human Esophagus	16	0.1993	0.0608	1.0756	0.2956	1.6632	0.5309	46.1425	11.1361	70.1833	21.0146	0.3942	0.2208
6	5	Cryo-Ablated Human Squamous Epithelium Manual	8	0.3781	0.2166	0.7665	0.2015	1.6522	0.3404	69.3636	43.2983	141.4040	60.9934	0.9794	0.4459
7	6	Cryo-Ablated Swine Diaphragm	58	0.1858	0.0824	0.6301	0.2503	0.8021	0.3449	24.1085	15.0769	31.5931	17.8024	0.6629	0.3949
8	7	Cryo-Ablated Swine Diaphragm Manual	25	0.1013	0.0387	1.8385	0.8437	2.5278	1.1956	54.1489	27.5617	67.2937	37.0989	0.1224	0.0445
9	8	Cryo-Ablated Swine Esophagus	16	0.5929	0.1702	1.4111	0.2671	1.8404	0.3319	208.8023	83.9277	260.1545	92.3517	0.6695	0.2048
10	9	Cryo-Ablated Swine Esophagus Manual	8	0.5150	0.1464	1.8486	0.5506	2.5741	0.5245	213.4147	64.5272	274.5535	76.2793	0.5280	0.2103
11	10	EtOH-Ablated Human Vastus Lateralis	2	0.1003	0.0049	0.5542	0.2037	0.8249	0.2233	16.7105	7.8255	25.7621	10.5752	0.4120	0.0257
12	11	EtOH-Ablated Swine Diaphragm	34	0.1827	0.0829	0.7085	0.2096	1.0071	0.3606	38.8015	24.1144	55.6371	39.4815	0.3852	0.1568
13	12	EtOH-Ablated Swine Esophagus	32	0.4826	0.1893	1.0517	0.1794	1.4834	0.2863	128.4547	62.7743	177.0754	81.5882	0.7128	0.2423
14	13	EtOH-Ablated Swine Trabeculae	23	0.1932	0.0931	1.0100	0.3440	1.2773	0.3870	64.8409	46.5131	82.5858	55.2193	0.2666	0.1282
15	14	HIFU-Ablated Human Esophagus	8	0.3189	0.1064	0.9535	0.2588	1.6407	0.4595	74.0712	33.8573	133.4991	55.8577	0.5901	0.1677
16	15	HIFU-Ablated Human Trabeculae	6	0.3861	0.1089	0.8285	0.2816	1.2215	0.3004	86.5987	28.4575	116.2640	37.5634	0.8739	0.5628
17	16	HIFU-Ablated Swine Diaphragm	49	0.1728	0.0744	0.7784	0.2849	1.1205	0.5019	32.8586	25.8337	46.9847	33.9354	0.4859	0.2900
18	17	HIFU-Ablated Swine Esophagus	15	0.6034	0.1799	0.9877	0.1676	1.2275	0.2982	146.2820	50.8412	194.7083	73.6505	0.9574	0.2767
19	18	Krebs-Injected Swine Diaphragm	30	0.2152	0.0749	0.8940	0.1793	1.2259	0.2409	47.1391	17.7803	67.8749	29.0318	0.4073	0.1486
20	19	Krebs-Injected Swine Esophagus	16	0.5972	0.1166	1.4484	0.2968	1.9275	0.3586	211.4609	62.8552	279.5098	79.3904	0.6568	0.1905
21	20	Microwave-Ablated Human Vastus Lateralis	12	0.1022	0.0465	0.5075	0.1872	0.6734	0.2816	13.7281	9.6930	18.7865	13.8787	0.3707	0.1709
22	21	Microwave-Ablated Swine Diaphragm Manual	16	0.2351	0.1065	1.1834	0.3506	1.7835	0.5175	86.8545	55.0204	123.3605	70.9502	0.2881	0.1396
23	22	Microwave-Ablated Swine Esophagus	16	0.6322	0.1817	1.3025	0.3267	1.8000	0.4678	210.3245	81.4199	271.6986	102.0898	0.7668	0.2335
24	23	NaCl-Ablated Human Vastus Lateralis	2	0.0530	0.0130	0.4758	0.0293	0.5968	0.1069	4.8130	1.0532	8.2084	3.7259	0.2425	0.0788
25	24	NaCl-Ablated Swine Diaphragm	21	0.2108	0.0740	0.8803	0.2035	1.1963	0.2777	50.7658	23.8252	67.1144	29.7492	0.3748	0.1338
26	25	NaCl-Ablated Swine Esophagus	16	0.5033	0.1344	1.2581	0.2123	1.6224	0.3616	156.7233	63.0207	208.4701	88.3197	0.6246	0.1021
27	26	Non-Ablated Human Aorta	27	0.8273	0.2764	1.3497	0.3612	1.6811	0.4924	253.6208	120.8743	355.5709	170.3970	1.2461	0.3949
28	27	Non-Ablated Human Esophagus	73	0.1995	0.1131	1.5555	0.5089	2.2026	0.6901	63.0905	35.6432	92.3348	49.2330	0.2759	0.1883
29	28	Non-Ablated Human Lungs	5	0.1936	0.0818	0.7847	0.1569	1.1533	0.4197	38.9630	20.7465	50.7770	28.0055	0.4913	0.1928
30	29	Non-Ablated Human Pericardium	21	5.1777	2.1895	0.7614	0.3355	1.0705	0.4433	1225.9000	827.2746	1545.5000	998.6706	10.5539	3.9687
31	30	Non-Ablated Human Squamous Epithelium	24	0.5158	0.2374	0.8394	0.2983	1.5944	0.6065	133.9773	67.2059	199.3178	117.9189	1.1182	0.6945
32	31	Non-Ablated Human Trabeculae	22	0.2078	0.2932	0.8040	0.2752	1.1697	0.4306	47.4752	55.6041	64.2484	70.9153	0.2732	0.1705
33	32	Non-Ablated Human Trachea	3	2.8185	1.9344	1.7396	1.0761	2.1019	1.1371	1649.5000	1972.2000	2154.5000	2536.6000	2.3502	0.2080
34	33	Non-Ablated Human Vastus Lateralis	24	0.1132	0.0716	0.8497	0.4231	1.3048	0.6770	25.9326	21.3254	44.4887	43.3419	0.2834	0.2290
35	34	Non-Ablated Swine Aorta	120	1.0988	0.4013	1.0166	0.2851	1.2157	0.4092	230.4118	127.6409	304.9620	182.8668	2.4301	1.1372
36	35	Non-Ablated Swine Diaphragm	327	0.1732	0.0830	1.0971	0.3870	1.5894	0.6487	43.6015	31.0626	65.7510	50.2313	0.3432	0.1961
37	36	Non-Ablated Swine Esophagus	347	0.4695	0.1719	1.3376	0.4021	1.7497	0.5650	138.6364	66.7472	178.7045	84.3734	0.6979	0.3957
38	37	Non-Ablated Swine Lungs	33	0.1096	0.0544	1.0271	0.3850	1.8061	0.6668	25.9422	15.2773	47.5768	23.1502	0.2218	0.1378
39	38	Non-Ablated Swine Pericardium	26	6.1852	2.7884	0.6760	0.2488	0.8810	0.2500	1414.0000	1094.2000	1733.4000	1207.5000	16.0713	5.8072
40	39	Non-Ablated Swine Rectus Abdominus	74	0.1311	0.0730	0.8240	0.3144	1.1241	0.4443	23.5132	13.8973	35.5046	28.0866	0.3226	0.1711
41	40	Non-Ablated Swine Spinal Cord	2	0.0320	0.0121	0.7001	0.0583	1.3962	0.4161	7.0370	4.0290	10.4617	3.5931	0.0637	0.0208
42	41	Non-Ablated Swine Squamous Epithelium	26	0.7814	0.3407	1.5446	0.3380	1.9342	0.3779	339.9134	203.5549	407.7290	230.5105	0.7505	0.2478
43	42	Non-Ablated Swine Trabeculae	117	0.2283	0.1530	1.0158	0.3589	1.4119	0.5375	67.0822	46.3033	91.9007	64.9240	0.3602	0.2814
44	43	Non-Ablated Swine Trachea	43	1.7786	0.8932	0.6838	0.3660	0.8789	0.5196	322.5143	207.7289	409.4573	261.0601	4.6487	2.5973
45	44	Non-Ablated Swine Vastus Lateralis	10	0.0702	0.0178	0.5989	0.2475	0.8672	0.2936	16.5065	9.3449	21.2811	9.9080	0.1331	0.0612
46	45	RF-Ablated Human Esophagus	16	0.5126	0.1912	1.4748	0.2707	2.0006	0.5218	167.9645	69.8951	213.7736	79.6083	0.6183	0.2355
47	46	RF-Ablated Human Esophagus Manual	12	0.7256	0.2135	1.4070	0.1552	2.0910	0.4910	251.7574	73.9998	342.4986	95.8790	0.7643	0.2489
48	47	RF-Ablated Human Squamous Epithelium Manual	12	1.0530	0.6244	1.2576	0.4058	1.9177	0.4825	497.2899	488.2691	663.9057	493.7316	1.2288	0.4452
49	48	RF-Ablated Human Trabeculae	16	0.1885	0.1240	1.0392	0.3740	1.3567	0.6524	54.6338	42.9662	73.4772	65.0764	0.2865	0.1730
50	49	RF-Ablated Human Vastus Lateralis	14	0.0651	0.0364	0.6239	0.3059	0.9321	0.3809	12.4940	7.8560	18.5954	11.9689	0.1854	0.1104
51	50	RF-Ablated Swine Diaphragm	111	0.1597	0.0796	0.9015	0.2975	1.2031	0.4173	35.0616	22.2027	47.7570	29.8669	0.3288	0.2081
52	51	RF-Ablated Swine Diaphragm Manual	25	0.1660	0.0639	0.9877	0.3650	1.3694	0.4839	55.6966	30.0048	75.4493	38.3285	0.2427	0.1525
53	52	RF-Ablated Swine Esophagus	32	0.5797	0.1668	1.1469	0.2434	1.5999	0.3793	152.4346	65.3518	200.5924	77.0522	0.8934	0.2935
54	53	RF-Ablated Swine Esophagus Manual	15	0.5783	0.1144	1.8752	0.4086	2.3076	0.4497	301.3282	79.8425	358.6813	95.7056	0.4513	0.1354
55	54	RF-Ablated Swine Trabeculae	7	0.3688	0.1443	1.1755	0.2804	1.5344	0.4893	129.2193	55.2176	165.7634	63.5499	0.4815	0.3198
56	55	Study-Control Human Esophagus	7	0.2830	0.0635	1.0678	0.2580	1.8742	0.3816	74.1247	25.8551	116.5387	40.8906	0.4495	0.1009
57	56	Study-Control Human Trabeculae	2	0.1911	0.0171	0.5908	0.0238	1.6827	0.8800	37.9349	5.7480	72.1628	20.1964	0.3402	0.0758
58	57	Study-Control Human Vastus Lateralis	6	0.0867	0.0445	0.3671	0.1556	0.5927	0.2722	7.7136	3.7580	13.3566	8.2387	0.4133	0.2413
59	58	Study-Control Swine Diaphragm	38	0.1992	0.1499	0.7141	0.3699	0.9229	0.5013	30.1518	23.2297	40.9799	33.3842	0.5885	0.3919
60	59	Study-Control Swine Esophagus	3	0.5375	0.1094	1.0316	0.2915	1.4642	0.4110	130.6403	57.9100	194.1316	63.6180	0.8198	0.1197
61	60	Study-Control Swine Trabeculae	10	0.2964	0.1250	1.2227	0.4084	1.5773	0.4500	109.3351	72.1392	141.7832	87.7023	0.3471	0.1389
62	61	Urea-Ablated Human Vastus Lateralis	2	0.0886	0.0115	0.5357	0.0502	0.8123	0.0779	10.4834	0.5040	19.5978	2.8400	0.2701	0.0300
63	62	Urea-Ablated Swine Diaphragm	25	0.1947	0.0511	0.8535	0.1825	1.2808	0.3372	46.6362	14.8571	67.5089	25.9743	0.3840	0.1056
64	63	Urea-Ablated Swine Esophagus	32	0.5659	0.2575	1.3143	0.2876	1.6936	0.3241	182.2017	89.0045	224.2774	108.5841	0.7057	0.3138
65	64	Urea-Ablated Swine Trabeculae	8	0.2272	0.0665	1.1077	0.2558	1.6350	0.3729	75.5967	26.7586	107.3392	36.5676	0.2441	0.0870

Table 1. *List of tissues under native and ablated conditions whose biomechanical properties have been evaluated in this investigation.*

RESULTS

- Biomechanical properties of **2180** samples of **19** different tissues *(8 human and 11 swine)* have been studied
- 8 human tissues: Aorta, Cardiac Trabeculae, Esophagus, Esophageal Squamous Epithelium, Lungs, Pericardium, Trachea, Vastus Lateralis
- 11 swine tissues: Aorta, Cardiac Trabeculae, Diaphragm, Esophagus, Esophageal Squamous Epithelium, Lungs, Pericardium, Rectus Abdominus, Spinal Cord, Trachea, Vastus Lateralis
- Comparative assessment of 2180 samples along with their stretch characteristic data is shown in **Table 1** and an example in **Figure 5**
- During the stretch, the tissue sample could avulse at any location along the longitudinal axis of the muscle bundle; hence based on where the tissue avulsed, five different avulsion locations were identified *(i.e.* ***1*** *= top-suture,* ***2*** *= center-top,* ***3*** *= center,* ***4*** *= center-bottom, and* ***5*** *= bottom-suture)* which were recorded for each sample that is graphically shown in **Figure 6**
- Avulsion Force and Elastic Modulus for diaphragmatic and esophageal samples is shown in **Figure 7** and **Figure 8**, respectively

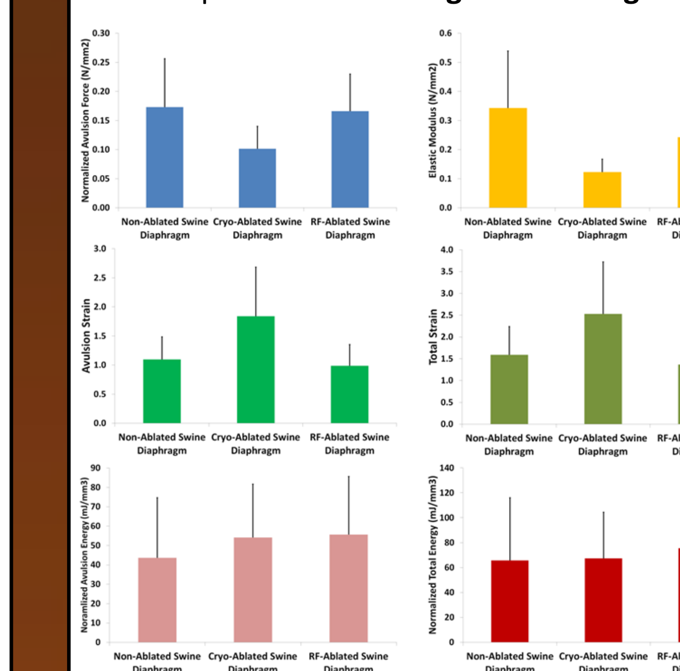

Figure 5. *Stretch characteristics*

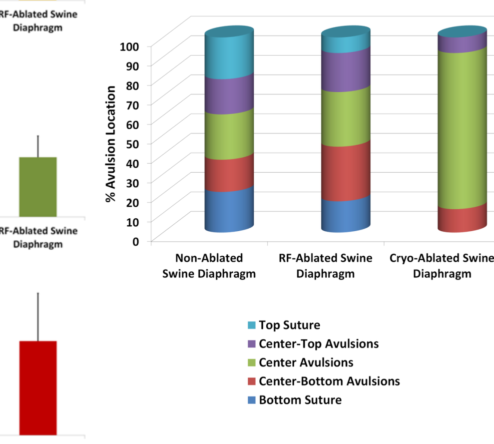

Figure 6. *Avulsion location*

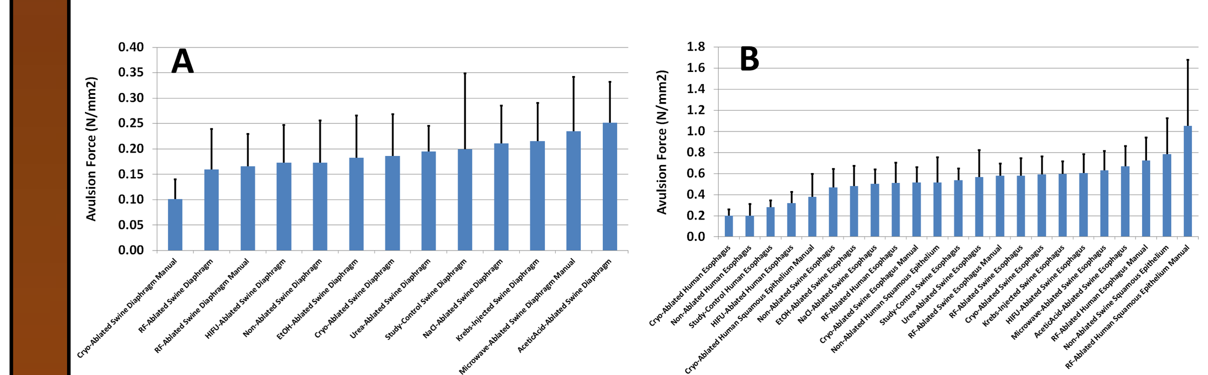

Figure 7: *Normalized avulsion force for diaphragmatic samples* ***(A)*** *and esophageal samples* ***(B)*** *under native and ablated conditions.*

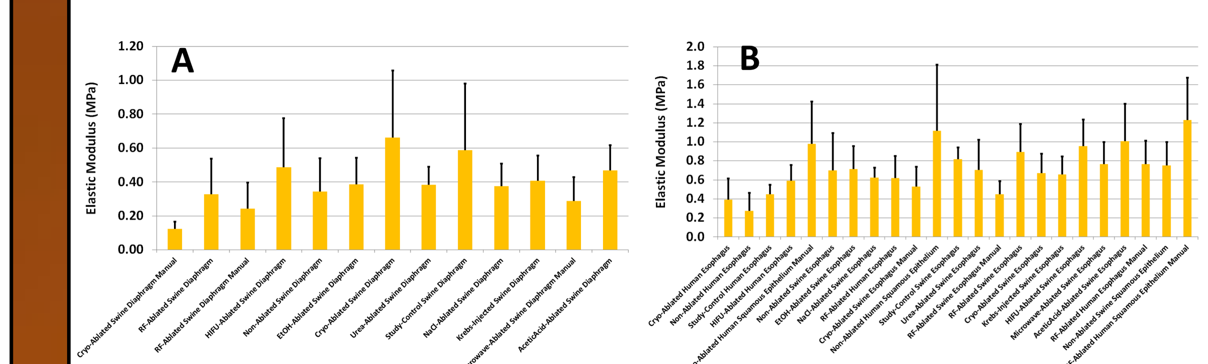

Figure 8: A: *Elastic modulus of diaphragmatic samples (A) and esophageal samples (B) under native and ablated conditions.*

INTERPRETATION

- We have developed methodologies that can be reliably used to assess biomechanical properties of a wide range of both swine and human tissues under uniaxial stress
- The stress-strain relationships developed in this investigation can not only be used to measure intra- and inter-tissue variability, but also provide insights in the mechanisms by which ablations/diseases affect the mechanical behavior of tissues
- Although our study approach may have a few limitations *(only uniaxial assessment)*, a comparative understanding of tissue properties is of importance from the perspective of developing realistic frameworks for considering device-tissue interactions that can aid in novel medical device design

REFERENCES and ACKNOWLEDGEMENTS

1. Khanafer K, Duprey A, Zainal M, Schlicht M, Williams D, Berguer R. Determination of the elastic modulus of ascending thoracic aortic aneurysm at different ranges of pressure using uniaxial tensile testing. J Thorac Cardiovasc Surg. 2011 Sep;142(3):682-6.
2. Duprey A, Khanafer K, Schlicht M, Avril S, Williams D, Berguer R. In vitro characterisation of physiological and maximum elastic modulus of ascending thoracic aortic aneurysms using uniaxial tensile testing. Eur J Vasc Endovasc Surg. 2010 Jun;39(6):700-7.
3. García Páez JM, Jorge E, Rocha A, Maestro M, Castillo-Olivares JL, Millan I, Carrera A, Cordon A, Tellez G, Burgos R. Mechanical effects of increases in the load applied in uniaxial and biaxial tensile testing: Part I. Calf pericardium. J Mater Sci Mater Med. 2002 Apr;13(4):381-8.

We would like to thank the donors and their families for their generous gifts as well as Lifesource for their contributions. Thanks are also extended to volunteers at the Visible Heart Laboratory for their help with experiments. This study was supported in part by "Minnesota Muscle Training Program" NIH 2T32 AR007612.